Supporting Information

Enhancing Performance of Organic Phototransistors by a Sandwich-Heterostructure

*Chi Yan,[a] Qi Wang,[a] Weijie Gong,[a] Jie Lu,[a] Yao Yin,[a] Chuan Xiang,[a] Di Xue,[*a] Zi Wang,[b] Lizhen Huang[*a] and Lifeng Chi[*a]*

a. Institute of Functional Nano & Soft Materials (FUNSOM), Jiangsu Key Laboratory for Carbon-Based Functional Materials & Devices, Soochow University, 199 Ren'ai Road, Suzhou, 215123, Jiangsu, P. R. China.

E-mail: chilf@suda.edu.cn (LiFeng Chi), lzhuang@suda.edu.cn (Lizhen Huang), dixue0130@suda.edu.cn (Di Xue)

b. Suzhou Laboratory, Suzhou 215123, China

1. Experimental Section:

Film and Device Fabrication: The organic molecules C8-BTBT and DCV3T were purchased from Lumtec Company and used as received without further purification. Highly doped silicon (Si) wafers were used as substrates, with a 300 nm thick thermally grown silicon dioxide (SiO_2) layer (dielectric capacitance C_i=10 nFcm^{-2}) serving as the gate electrode and dielectric layer. All substrates were sonicated in acetone, ethanol, and deionized water for 20 minutes each, followed by drying under N_2. Then, the substrates were loaded into a vacuum chamber, and C8-BTBT thin films were deposited at room temperature under vacuum, followed by deposition of DCV3T thin films using a metal shadow mask. Deposition was carried out at pressures of 10^{-4}-10^{-5} Pa, with a deposition rate of 1 nm min^{-1}. A 40 nm thick layer of Ag was deposited on the organic films through a metal shadow mask at a deposition rate of 3 Å s^{-1}, forming the source/drain electrodes with channel lengths (L) and widths (W) of 50 and 1000 μm, respectively.

Characterization and Measurements: The morphology of the films was characterized by AFM with a Bruker Dimensional Icon in the tapping mode, in which the tapping mode used silicon cantilever with a spring constant of 40 N m^{-1}. X-ray diffraction (XRD) patterns were obtained using a D8 Discovery thin-film diffractometer (λ = 1.54056 Å) with operating voltages of 40 kV and currents of 40 mA. The UV-vis absorption spectra of a series of thin films were obtained on a Perkin Elmer Lambda 950 spectrophotometer. The stable photoluminescence (PL) spectra were recorded using a fluorescence spectrometer (NIR-VIS, FL3), where the spot width and diameter of the sample illuminated by the xenon lamp are approximately 2 mm. The XPS (Al Kα, 1486.7 eV) and UPS (He Iα,21.22 eV) measurements were characterized by a monochromatized light source in a customized SPECS photoelectron spectroscopy system (base pressure:2×10^{-10} mbar). The SECO (to determine the VL) was measured in normal emission with bias potential of -3 V. The electrical and optoelectronic properties of the devices were measured under both air and vacuum conditions by using a semiconductor parameter analyzer (Keithley 4200) integrated with a high-vacuum probe station (Lake Shore). Monochromatic light of different wavelengths was generated using commercial light-emitting diode (LED) sources (CEAULIGHT CEL-LEDS35) and LED light sources where the diameter of the 365 nm lamp tube used is 0.8 mm. According to the distance between the lamp tube and the sample, the light spot area of the light source on the sample surface is 2.82 cm^2.

The *SS* parameter of transistors determines the gate voltage (V_G) necessary to improve drain-source current (I_{DS}) by 1 order of magnitude. By this definition, the SS can be calculated as:

$$SS = \frac{dV_G}{dlog(I_{DS})}$$

The maximum density of the interfacial traps (N_{trap}) resulting from the defects can be calculated through the following equation:

$$N_{trap} = \left\{\frac{Sloge}{k_BT/q} - 1\right\}\cdot\frac{C_i}{q}$$

Where e is the Euler number, k_B represents the Boltzmann constant, q represents the elementary charge, and T represents the absolute temperature.

The photosensitivity (P), photoresponsivity (R), and detectivity (D^*) of OPTs are extracted using the following equations:

$P = I_{ph}/I_{drak} = (I_{ill} - I_{dark})/I_{dark}$

Where I_{dark} and I_{ill} are the drain current at the same drain and gate voltages in the dark and under illumination, respectively; and I_{ph} is the difference between I_{dark} and I_{ill}.

$R = I_{ph}/P_{opt} = (I_{ill} - I_{dark})/(P_{inc}A)$

Where I_{dark} and I_{ill} are the drain current at the same drain and gate voltages in the dark and under illumination, respectively; P_{opt} and P_{inc} are the incident light intensity and incident light power density and A is the area of the illuminated channel.

$$D^* = RA^{1/2}/i_n$$

Where R is photoresponsivity, A is the area of the illuminated channel, in is the measured noise. The specific detectivity (D^*) are adopted to represent the detection ability of minimum optical signal.

2. Additional data

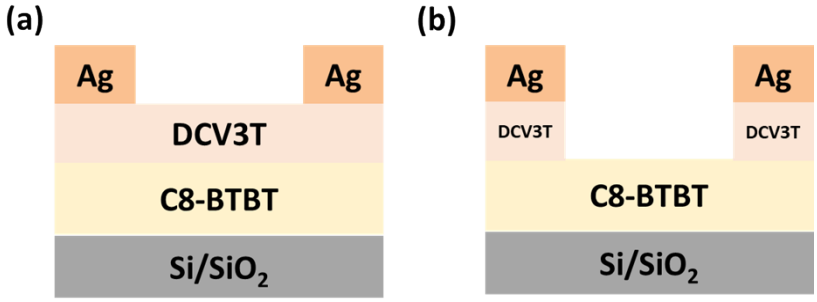

Figure S1. Schematic diagrams of transistor structures: (a) C8-BTBT/DCV3T planar heterostructure OPTs; (b) C8-BTBT/DCV3T-sandwich heterostructure OPTs.

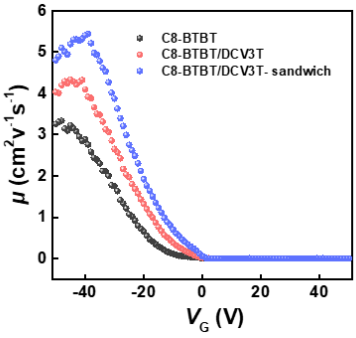

Figure S2. (a) Variation curves of the mobility μ of three types of organic field-effect transistors (OFETs) with respect to the gate voltage V_{G}.

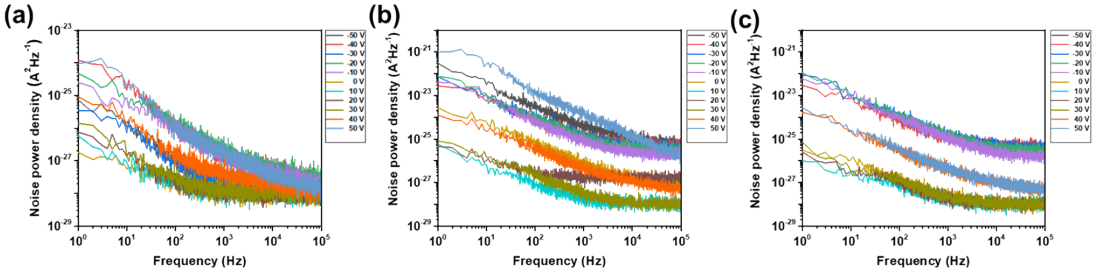

Figure S3. Frequency-dependent noise spectra at V_{D} = 0V for various gate voltages (a) C8-

BTBT OPTs; (b) C8-BTBT/DCV3T planar heterostructure OPTs; (c) C8-BTBT/DCV3T-sandwich heterostructure OPTs.

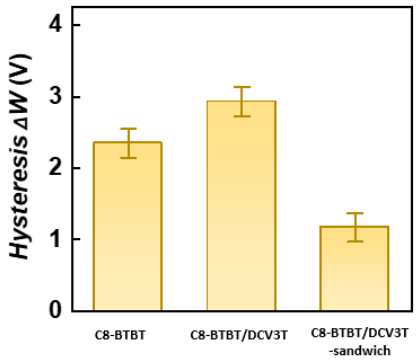

Figure S4. Hysteresis window ΔW of three types of organic field-effect transistors.

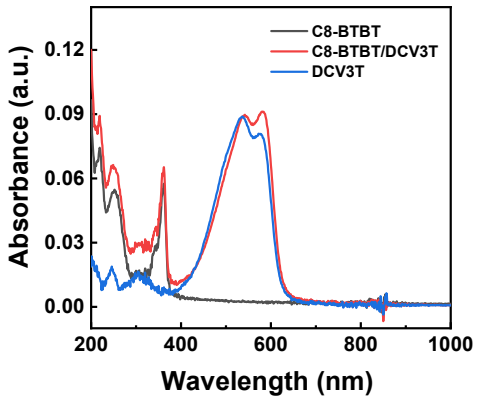

Figure S5. Ultraviolet absorption spectra of organic heterostructure thin films.

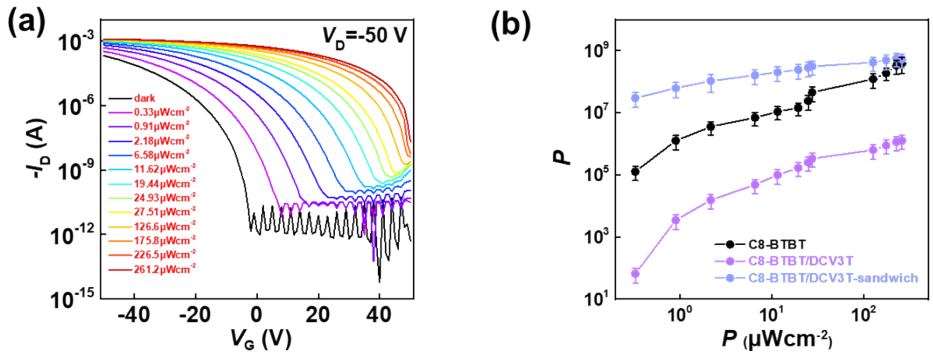

Figure S6. (a) Transfer curves of single-component C8-BTBT organic phototransistors (OPTs) under different light intensities; (b) Comparison of photosensitivity *P* for three types of OPTs.

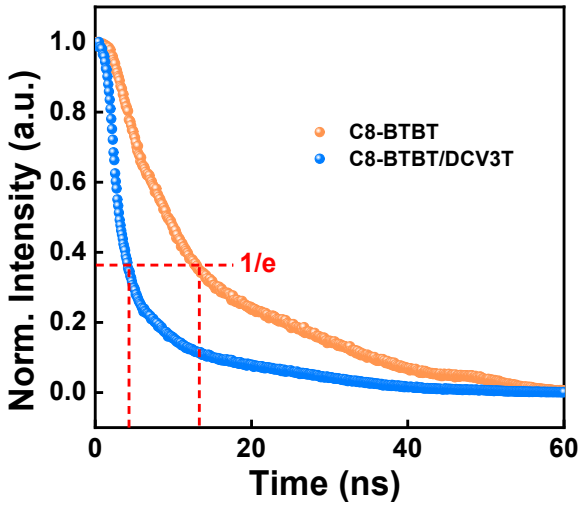

Figure S7. Time-resolved photoluminescence (TRPL) spectra of C8-BTBT and C8-BTBT/DCV3T thin films.

Table S1. Comparison of Electrical Performance Parameters of Transistors with Different Structures.

	μ_{eva} ($cm^2V^{-1}s^{-1}$)	V_{th} (V)	I_{on}/I_{off}	*SS* (V dec^{-1})	N_{trap} ($cm^{-2}eV^{-1}$)
C8-BTBT	2.45	-16.97	10^8	0.53	4.93×10^{11}
C8-BTBT/DCV3T	3.78	-15.98	10^6	3.61	3.72×10^{12}
C8-BTBT/DCV3T-sandwich	4.12	-16.73	10^8	0.57	5.35×10^{11}

Table S2. Performance comparison of our work with previously reported typical planar heterojunction phototransistors.

Structure	μ / $cm^2V^{-1}s^{-1}$	I_{off}	*P*	*R* / A/W	D^*	*Ref.*
PBTT/MoO_3/PQDs/PLA	0.36	10^{-11}	1.5×10^4	2.1×10^4	10^{15}	1
C8-BTBT 1D arrays	13.52	10^{-12}	2.5×10^7	8.8×10^4	10^{15}	2
C8-BTBT/TFT-CN	0.91	10^{-13}	1.9×10^8	4.3×10^3	10^{17}	3
C8-BTBT/$(BA)_2(MA)Pb_2I_7$	1.99	10^{-11}	---	5.87×10^2	10^{12}	4
F_{16}CuPc/Rub	3.5	10^{-10}	10^2	2.2×10^4	10^{12}	5
C_{60}/Rub	2.7	10^{-10}	10^7	9.2×10^3	10^{15}	
PTCDA/PMMA	0.02	10^{-12}	---	1.8×10^2	10^{11}	6
Pentacene/PbPc/C_{60}	2.4×10^{-2}	---	1.2×10^4	1.4×10^0	10^{11}	7
C8-BTBT/DCV3T-sandwich	4.12	10^{-12}	5.2×10^8	3.3×10^6	10^{17}	this work

1. Y. Gao, S. Sun, D. Qiu, Y.-M. Wei, M. Zhang, J. Liu, P. K. Chu, W.-L. You and J. Li, *ACS Photonics*, 2023, **10**, 764-771.
2. X. Deng, Y. Zhang, Y. Guo, X. Li, S. Yang, X. Zhu, H. Gao, J. Feng, Y. Wu and L. Jiang, *Advanced Materials Technologies*, 2022, **7**, 2101134.
3. X. Zhu, Y. Yan, L. Sun, Y. Ren, Y. Zhang, Y. Liu, X. Zhang, R. Li, H. Chen, J. Wu, F. Yang and W. Hu, *Adv Mater*, 2022, **34**, e2201364.
4. H. Sun, H. Liu, F. Liu, H. Liu, C. Jiang and Y. Zhang, *Advanced Materials Interfaces*, 2022, **9**, 2101850.
5. D. Xue, Q. Wang, M. Xie, W. Gong, Y. Zhang, Y. Yin, Y. Wei, J. Lu, J. Zhang, S. Duhm, Z. Wang, L. Chi and L. Huang, *Advanced Optical Materials*, 2023, **12**, 2302091.
6. F. Ling, Q. Du, Y. Zhang, X. Zheng, A. Wang, C. Zhu, W. Wang, F. Wang and S. Qin, *Organic Electronics*, 2024, **124**, 160942.
7. Y. Hu, Y. Wang, Y. Li and L. Zhang, *Applied Sciences*, 2023, **13**, 11850-11855.